Cell, Volume *134*

Supplemental Data

Global Mapping of the Topography and Magnitude of Proteolytic Events in Apoptosis

Melissa M. Dix, Gabriel M. Simon, and Benjamin F. Cravatt

Supplemental Experimental Procedures

Cell Culture and Induction of Apoptosis

Jurkat cells were grown at 37°C under 5% CO_2 in RPMI 1640 media supplemented with 10% fetal calf serum (FCS) and 2 mM glutamine. Before induction of apoptosis, Jurkat cells were seeded to a density of 1 x 10^6 cells/ml in RPMI 1640 media containing 10% heat-inactivated FCS and 2 mM glutamine. DMSO or staurosporine (1 μM final concentration, Sigma) was added and the cells were incubated for 4 hrs at 37°C under 5% CO_2. Induction of apoptosis was monitored by DNA fragmentation assay (Supplemental Figure 7A). Briefly, 1 x 10^6 cells were washed 3 times with phosphate buffered saline (PBS) and lysed in 400 μl of lysis buffer (100 mM Tris pH 8.0, 5 mM EDTA, 0.2% SDS, 200 mM NaCl). Cells were then incubated with 0.1 mg/ml RNaseA for 0.5 hr at 37°C and then proteinase K was added to a concentration of 0.3 mg/ml and samples were incubated overnight at 55°C with shaking. Genomic DNA was then precipitated with 1 volume of isopropanol and resuspended in 100 μl of dH_2O. 25 μl of DNA was visualized on a 1% agarose gel.

Preparation of Cell Lysates

Soluble and particulate fractions were prepared as previously described (Jessani et al., 2002). Briefly, cells were washed 3 times in cold PBS and resuspended in 200 μl of PBS containing protease inhibitors (complete EDTA-free protease inhibitor cocktail, Roche). Cells were then sonicated to lyse and centrifuged at 145,000 x g for 45 minutes. The supernatant was collected as the soluble fraction and the pellet was resuspended in PBS with protease inhibitors (referred to as the particulate fraction).

Immunoblot Analysis

The soluble fractions of both control and STS treated Jurkat cells were analyzed via western blotting using standard methods. Blots were probed with antibodies for caspase-3, PARP1, JMJD1B, MAP2K1, and MAP2K2 (Cell Signaling Technology, 9662, 9542, 2621, 9124, and 9125, respectively), Trim28 (Abcam, ab10484), Vimentin (Novus, NB120-15248), and PAK2 (AbD Serotec, AHP1191). All antibodies were polyclonal.

Sample Preparation, SDS-PAGE, and Mass Spectrometry

100 µg of each protein sample were separated via a 10% SDS-PAGE gel for 850 volt hours. The gel was washed in water and manually excised into 0.5 cm bands. Bands which corresponded to the migration of molecular-weight markers were noted and this information was used to estimate the molecular weights of proteins migrating in each band. Bands were subjected to in-gel trypsin digestion as previously described (Rosenfeld et al., 1992) with minor modifications. Briefly, bands were washed in 100 mM ammonium bicarbonate and proteins were reduced in 10 mM tris(2-carboxyethyl)phosphine (TCEP) at 65°C for 0.5 hr and then alkylated with 55 mM iodoacetamide in the dark for 0.5 hr. The bands were then dehydrated by washing in 50:50 acentonitrile:100 mM ammonium bicarbonate. Gel bands were then dried and resuspended in 40 µl of trypsin at 10 ng/µl. Upon re-swelling of the gel bands, 25 mM ammonium bicarbonate was added to a final volume of 200 µl and the gel bands were placed at 37°C overnight. Supernatants containing peptides were removed, and the gel bands were further extracted with 5% formic acid and acetonitrile. The pooled supernatant was dried and resuspended in 10 µl buffer A (95% H_2O, 5% acetonitrile, 0.1% formic acid) and pressure loaded onto a 100 µm (inner diameter) fused silica capillary column with a 5 µm tip that contained 10 cm of C18 resin (aqua 5µm, Phenomenex). LC-MS/MS analysis was performed on an LTQ ion trap mass spectrometer (ThermoFisher) coupled to an Agilent 1100 series HPLC. Peptides were eluted from the column using a 2-hour gradient of 5-100% Buffer B (Buffer B: 20% H_2O, 80% acetonitrile, 0.1% formic acid). The flow rate through the column was 0.25 µl/min and the spray voltage was 2.5 kV. The LTQ was operated in data-dependant scanning mode, with one full MS scan (400-1,800 m/z) followed by seven MS^2 scans of the n^{th} most abundant ions with dynamic exclusion enabled.

Replicates

All comparisons were performed with at least three biological replicates. For the control- and 4 hr datasets, an additional technical replicate was included to assess variability due to sample handling and preparation. Spectral counts for nearly all proteins from this dataset (99.3%) that were included in our quantitative analyses (having greater than 30 total spectral counts) were detected in all four replicates. Thus, all of the data presented in the paper represents quadruplicate analysis (3 biological replicates plus 1 technical replicate) except for the time-course study which was conducted with three biological replicates only. All data are presented +/- standard error of the mean. Analysis of the reproducibility of the data can be found in **Supplemental Figure 10**.

Data Collection and Analysis

Raw mass spectrometry data were stored in RAW files generated by XCalibur version 1.4 running on a ThermoFinnigan LTQ mass spectrometer. RAW files were converted to MS2 format using RAW-Xtract version 1.8 and these MS/MS data were searched using version 3.0 of the SEQUEST algorithm (Eng et al., 1994). SEQUEST searches were performed using a concatenated target/decoy non-redundant variant of the human IPI database version 3.33 (available for download at http://www.scripps.edu/chemphys/cravatt/protomap) allowing for differential methionine oxidation (+/- 16 amu) and requiring cysteines to be carboxyamidomethylated (+ 57 amu). SEQUEST data from each gel band were filtered and sorted with DTASelect version 1.9 (Tabb et al., 2002) using default settings except for the following switches: "-y 1 -Stn RKD -Stc RKD –p 1" which require peptides to be tryptic on at least one terminus and allows the other terminal residue to be lysine, arginine, or aspartate and places no requirement on the number of peptides per locus at this stage. Peptides in the +1, +2, and +3 charge-states were required to have minimum XCorr values of 1.8, 2.5, and 3.5, respectively. The minimum required deltaCN was 0.08.

The combined data from the analysis of the soluble fraction of the 4hr time-point consisted of 3989 distinct proteins, 1648 of which were detected with greater than 30 total spectral counts and were thus considered suitable for quantitative analysis. At this stage the false-positive rate was assessed according to established guidelines (Elias and Gygi, 2007) and found to be 0.53% implying that approximately 1 in 200 peptides were mis-assigned. DTASelect files from the 176 separate gel bands (control versus 4 hr staurosporine, 22 bands, 4 replicates) were then processed using three custom perl scripts. Sequence coverage maps were generated from DTASelect-filter.txt files using a custom perl

script (**coverage.pl**). Sequence coverage and spectral count data were then combined using another custom perl script (**protomap.pl**) which also applied one additional filtration step: two distinct peptides per locus were required to be present in any of the replicates for each band for a given condition or else the "singlet" peptides were discarded. The false-positive rate was re-assessed at this stage and found to be 0.0047% suggesting that a majority of the original false-positive identifications fell into this singlet peptide category. Finally, sequence-coverage maps and spectral-counting data were assembled into peptographs using a third custom perl script (**peptographer.pl**). For generation of each peptograph, spectral counts were averaged for each band and condition and displayed with error bars representing standard errors of the mean. Full datasets are available from our website (http://www.scripps.edu/chemphys/cravatt/protomap) as well as instructions for downloading and running these scripts.

Peptographic data was then examined using an additional script (**protosort.pl**) to identify proteins displaying altered migration between control, and STS-treated samples. This automatically-generated list was then manually pruned to remove apparent false-positives that appeared to represent artifacts of the sorting algorithm rather than bona fide cleavage events. Artifacts of the sorting-algorithm generally fell into one of three categories: (1) None of the peptides providing evidence of cleavage were unique. (2) Protein showed substantial break-down but did not display a significant difference between control- and apoptotic samples. (3) Evidence of cleavage is provided solely by two distinct peptides migrating faster than the parent species. [To be conservative in our interpretations, we did not designate cleaved proteins based on this criterion alone.] For proteins with high sequence-related homologues (>75% identity, e.g., MAP2K1 and MAP2K2), peptographs were generated exclusively from unique peptides.

Supplemental Figures

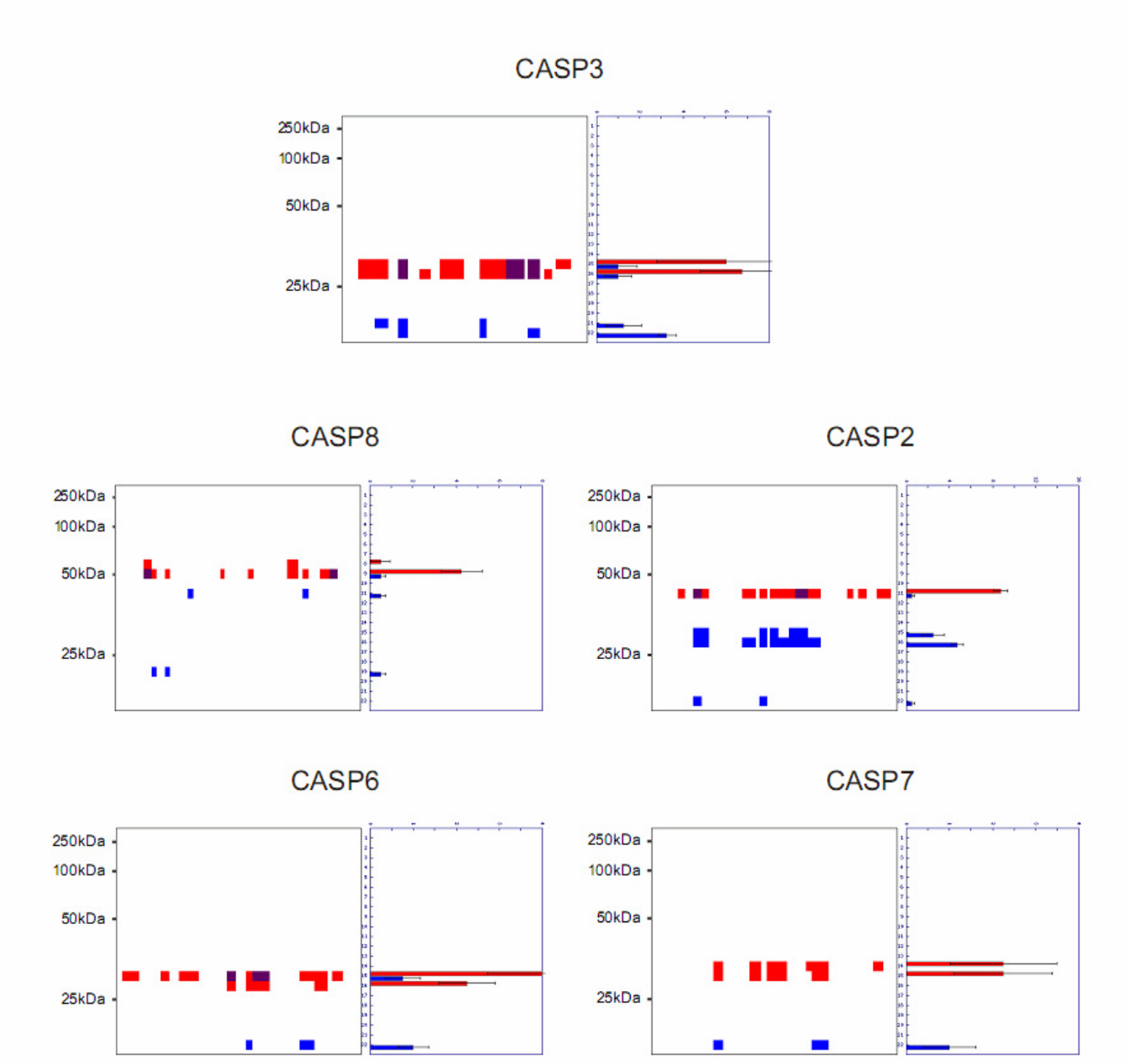

Figure S1. Peptographs for Members of the Caspase Family Detected by PROTOMAP in Control (Red) and Apoptotic (Blue) Cells

Note that all caspases show evidence of proteolytic cleavage in apoptotic cells.

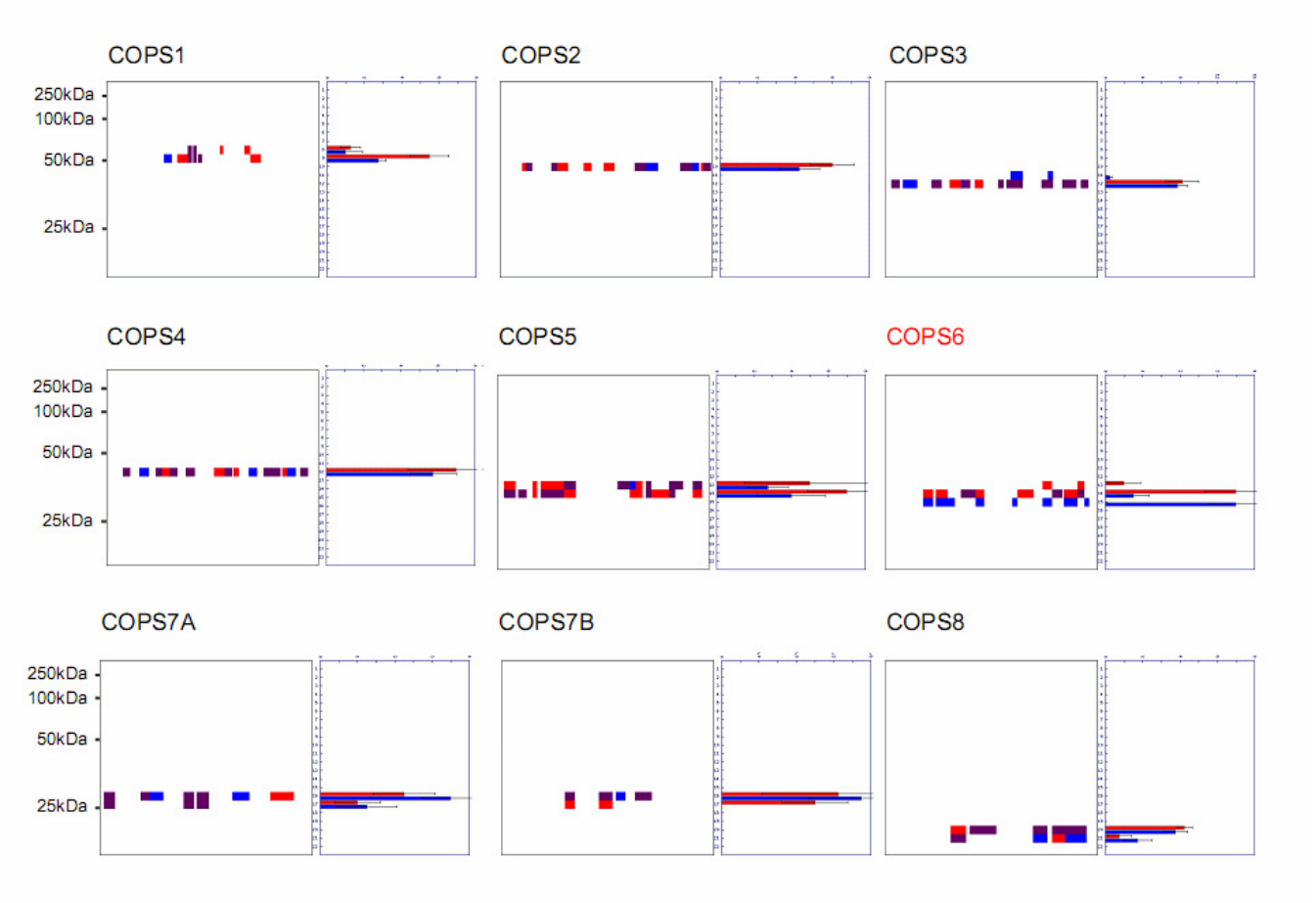

Figure S2. Peptographs for Members of the COP9 Signalsome Detected by PROTOMAP in Control (Red) and Apoptotic (Blue) Cells

Note that only COPS6 shows evidence of proteolytic cleavage in apoptotic cells.

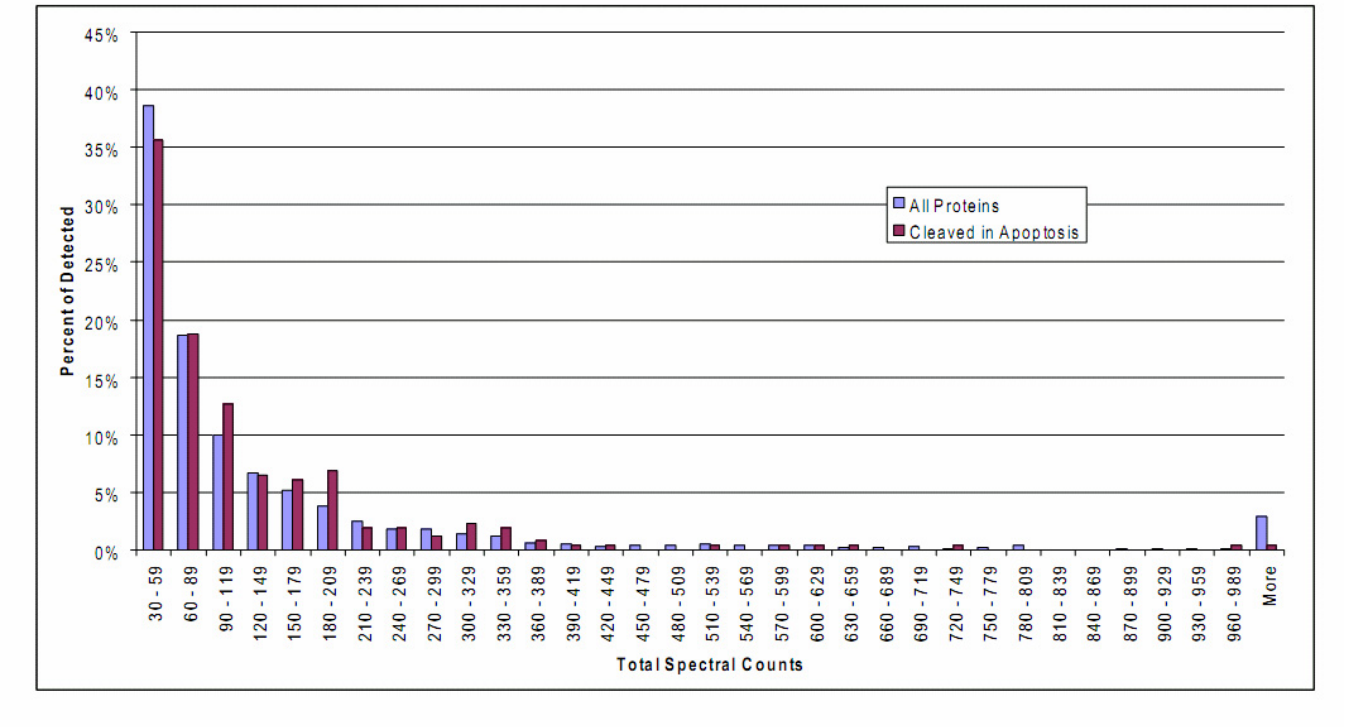

Figure S3. Comparison of the Spectral Count Distribution for Cleaved (Red) versus All (Cleaved + Noncleaved; Blue) Proteins

Note the overall similarity between the two distributions, indicating that cleaved proteins were detected with equivalent sensitivity to non-cleaved proteins.

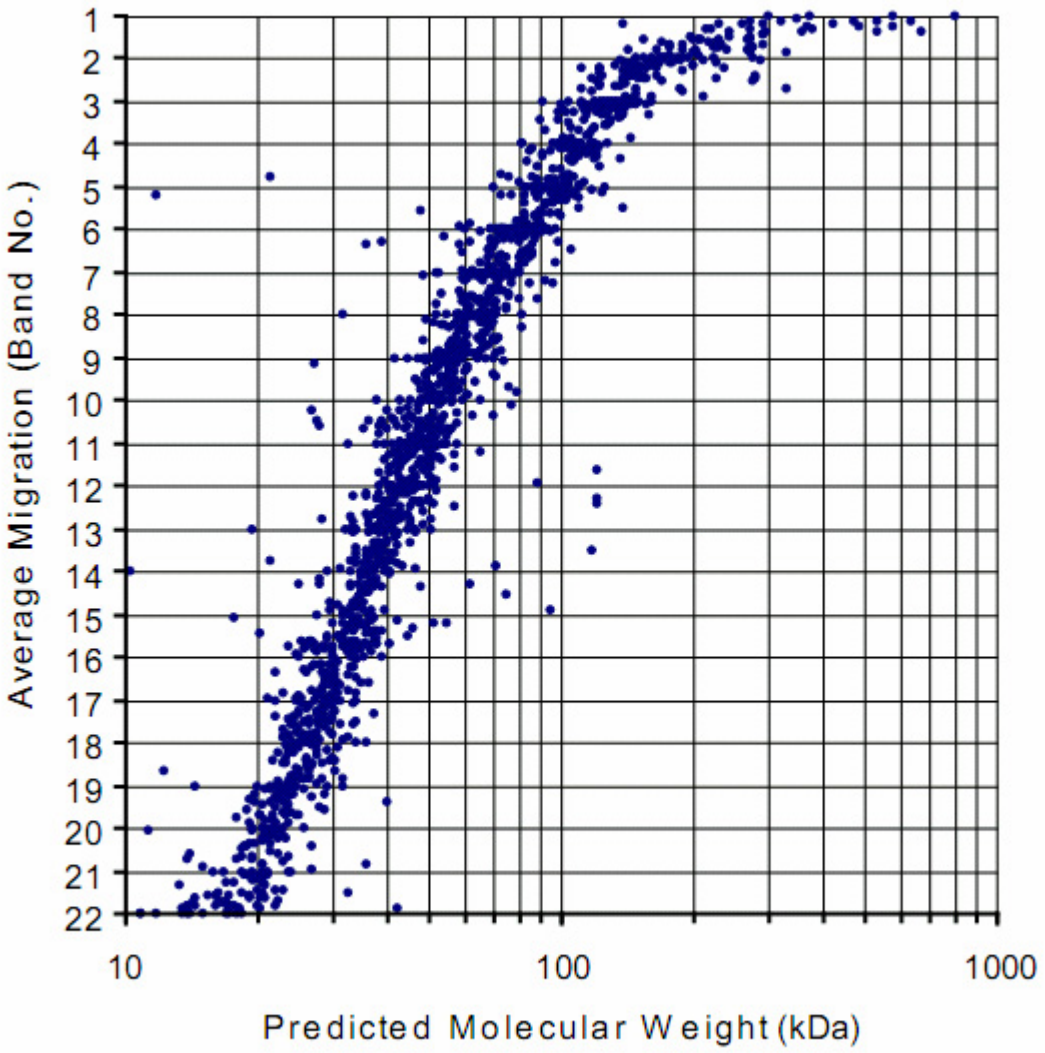

Figure S4. Scatter-Plot Showing Good Overall Correlation between the Average Rate of Gel-Migration (Band Number) versus Predicted Molecular Weight (kDa) for Proteins Identified by PROTOMAP

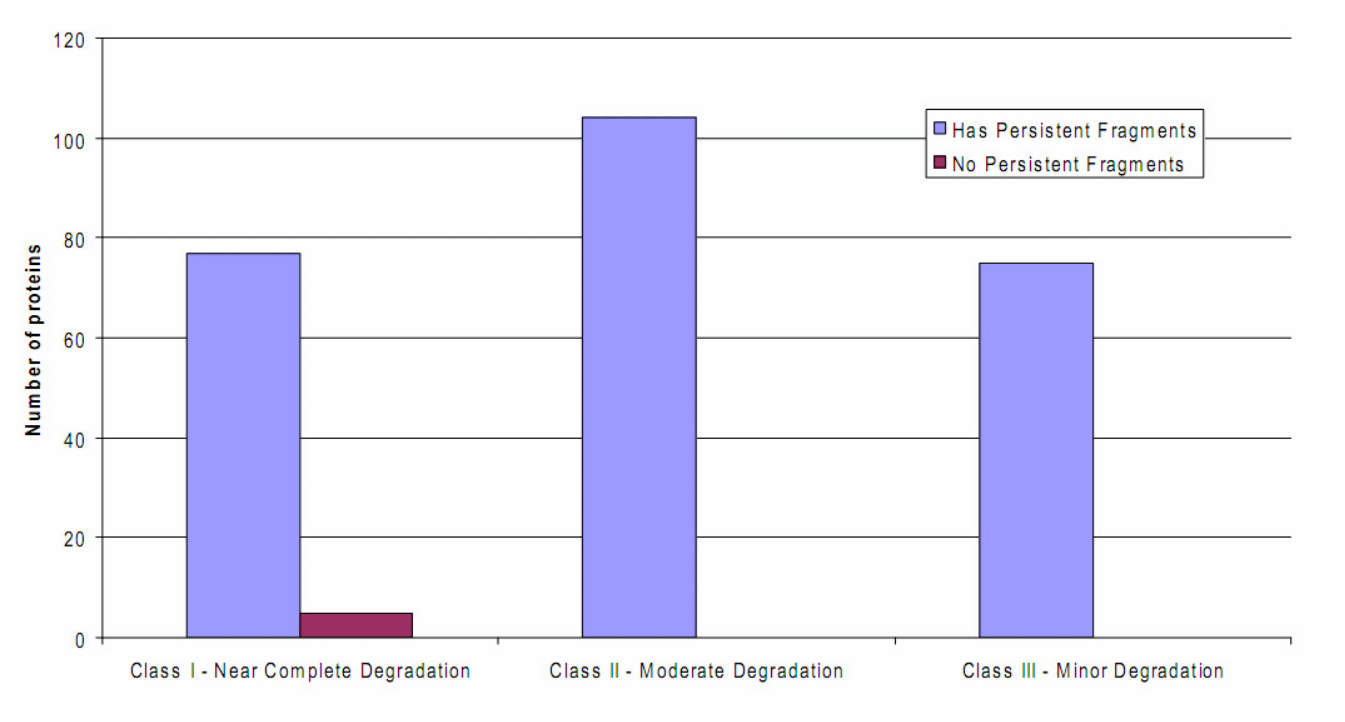

Figure S5. Bar Graph Showing that the Vast Majority of Cleaved Proteins in Apoptotic Cells, Regardless of Their Magnitude of Cleavage (Class I, II, or III), Showed Persistent Fragments

Supplemental Figure 6

A

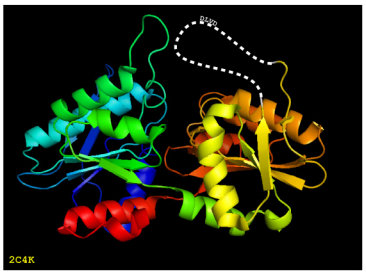

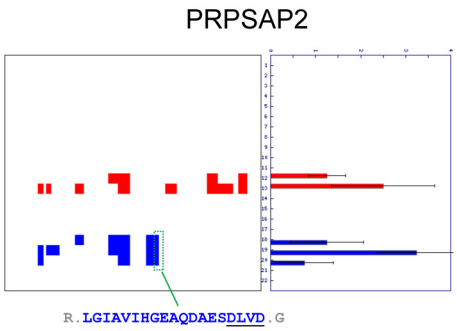

B

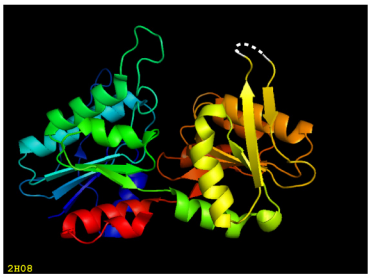

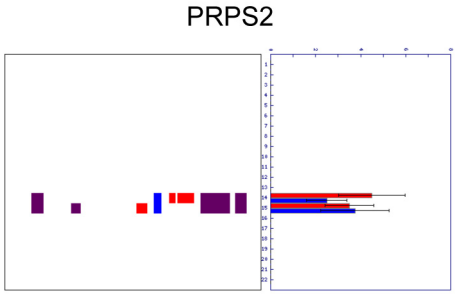

C

```
PRPSAP2 16  TKGGLVLFSANSNSSCMELSKKIAERLGVEMGKVQVYQEPNRETRVQIQESVRGKDVFII  75
            T   +VLFS +S+    +LS+++A+RLG+E+GKV   +  N+ET V+I ESVRG+DV+II
PRPS2   28  TMPNIVLFSGSSHQ---DLSQRVADRLGLELGKVVTKKFSNQETSVEIGESVRGEDVYII  84

PRPSAP2 76  QTVSKDVNTTIMELLIMVYACKTSCAKSIIGVIPYFPYSKQCKMRK-RGSIVSKLLASMM  134
            Q+   ++N  +MELLIM+ ACK + +  +  VIP FPY++Q K  K R  I +KL+A+M+
PRPS2   85  QSGCGEINDNLMELLIMINACKIASSRVTAVIPCFPYARQDKKDKSRAPISAKLVANML  144

PRPSAP2 135 CKAGLTHLITMDLHQKEIQGFFNIPVDNLRASPFLLQYIQEEIPDYRNAVIVAKSPASAK  194
              AG  H+ITMDLH  +IQGFF+IPVDNL A P +LQ+I+E I +++N +IV+     AK
PRPS2   145 SVAGADHIITMDLHASQIQGFFDIPVDNLYAEPAVLQWIRENIAEWKNCIIVSPDAGGAK  204

PRPSAP2 195 RAQSFAERLRLGIAVIHGEAQDAESDLVDGRHSPPMVRSVAAIHPSLEIPMLIPKEKPPI  254
            R  S A+RL +  A+IH E + A                              E   +
PRPS2   205 RVTSIADRLNVEFALIHKERKKA------------------------------NEVDRM  233

PRPSAP2 255 TVVGDVGGRIAIIVDDIIDDVDSFLAAAETLKERGAYKIFVMATHGLLSSDAPRRIEESA  314
             +VGDV  R+AI+VDD+ D   +   AA+ L   GA K++ + THG+ S  A  RI  +A
PRPS2   234 VLVGDVKDRVAILVDDMADTCGTICHAADKLLSAGATKVYAILTHGIFSGPAISRINNAA  293

PRPSAP2 315 IDEVVVTNTIPHEVQKLQCPKIKTVDISMILSEAIRRIHNGESMSYLFRNIGL  367
             + VVVTNTIP E +   C KI+ +DISMIL+EAIRR HNGES+SYLF ++ L
PRPS2   294 FEAVVVTNTIPQEDKMKHCTKIQVIDISMILAEAIRRTHNGESVSYLFSHVPL  346
```

D

Figure S6.

(A) The location of the site of caspase-cleavage is in an unstructured interdomain region of PRPSAP2 (as predicted from the crystal structure, PDB 2C4K). The peptograph for PRPSAP2 shows total degradation of the parent-species and a stable N-terminal persistent fragment. The closest neighbor of PRPSAP2, phosphoribosylpyrophosphate synthetase 2 (PRPS2) shares 44% overall homology with PRPSAP2 with the exception of an insertion that contains the site-of-cleavage (B, C). (D) Structure of PRPSAP2 showing the two domains that are separated by the interdomain linker-region and contains the site of caspase-cleavage.

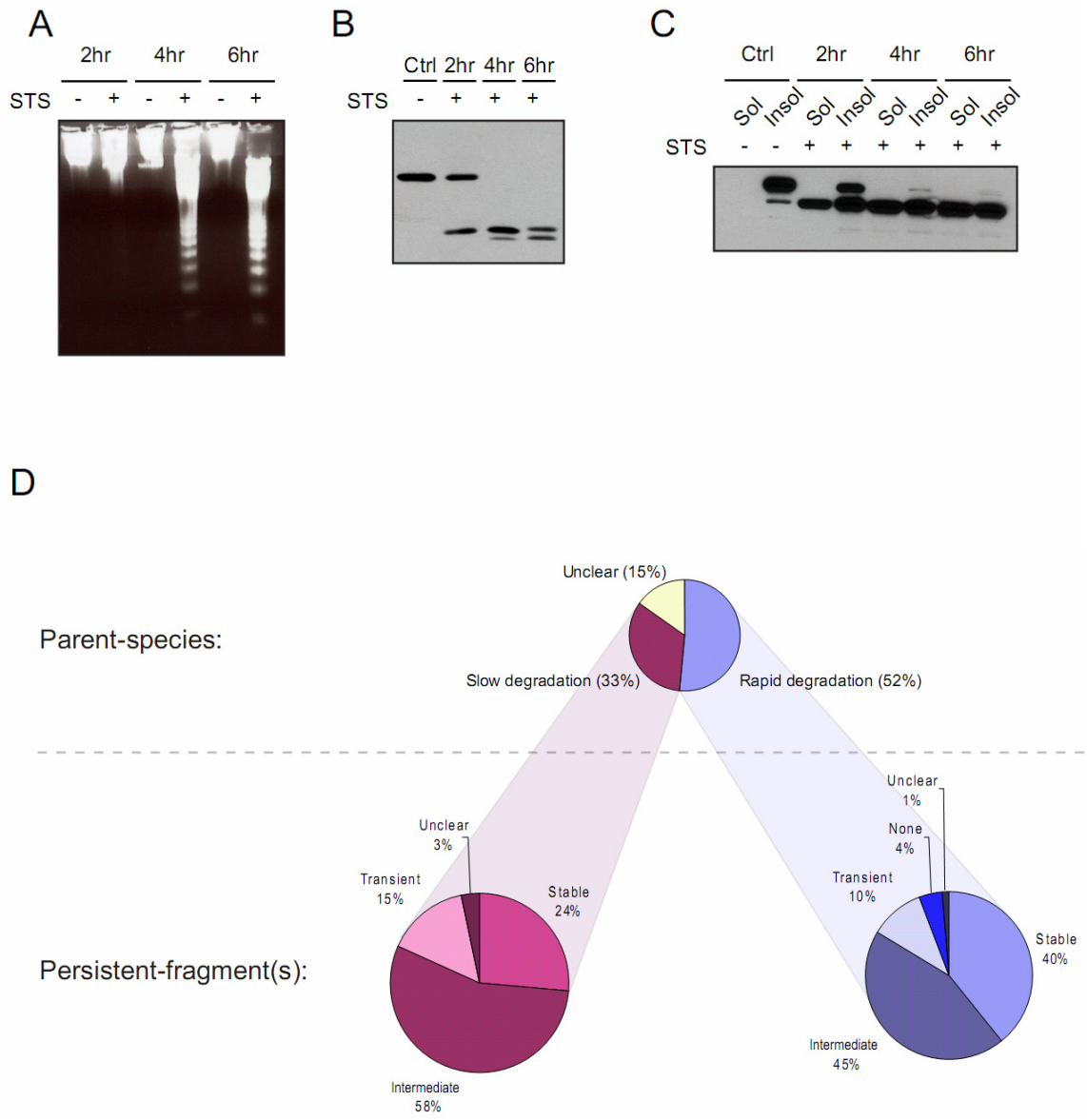

Figure S7. Temporal Analysis of Apoptosis

2, 4, and 6 hour time-points bracketing the early and late stages of apoptosis were chosen by monitoring DNA fragmentation (A), caspase 3 activation (B), and PARP1 cleavage (C). (D) Cleaved proteins were broken into categories based on their temporal stability. If >50% of the parent species was gone by 4 hours they were said to be Rapidly Degraded and if >50% of the parent species remained at 4 hours they were said to be degraded Slowly (see **Figure 6A**). Analysis of the persistent fragments in each category

revealed that a large majority of both Rapidly- and Slowly-degraded proteins displayed fragments that persisted for two (Intermediate) or three timepoints (Stable).

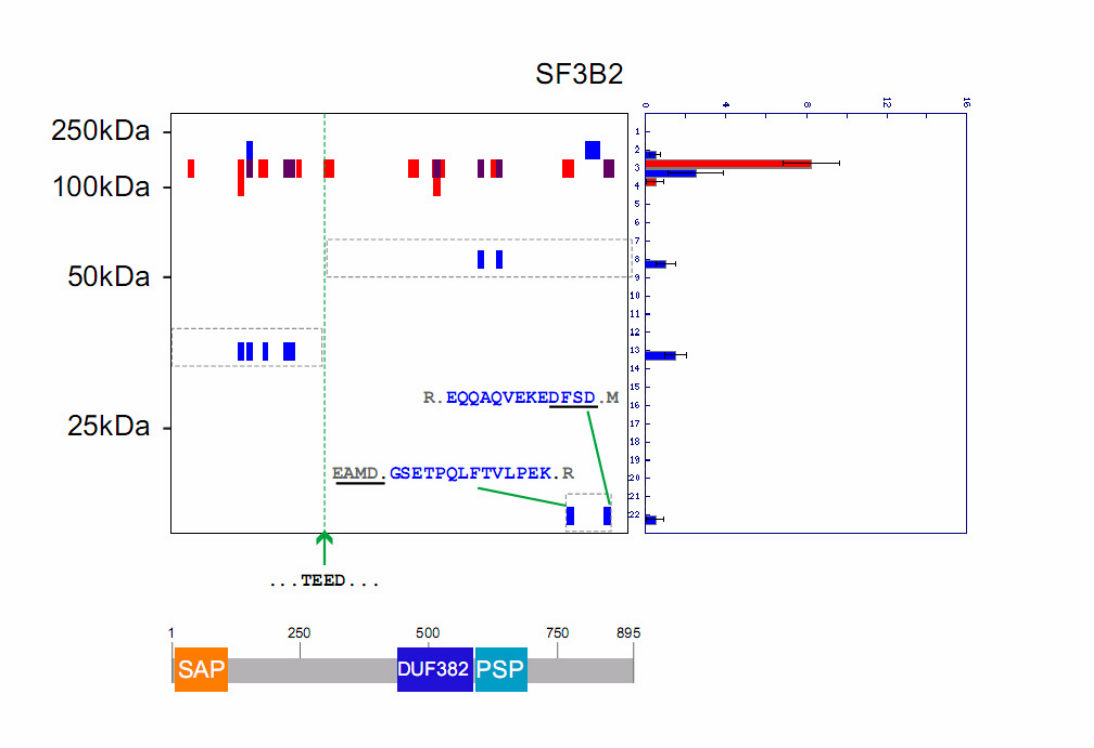

Figure S8. Peptograph of SF3B2 Showing Multiple Explicit Sites of Caspase Cleavage Identified by PROTOMAP, as well as an Implicit Site of Cleavage that Corresponds to a Cleavage Event Identified Previously by N-Terminal Labeling (Van Damme et al. 2005)

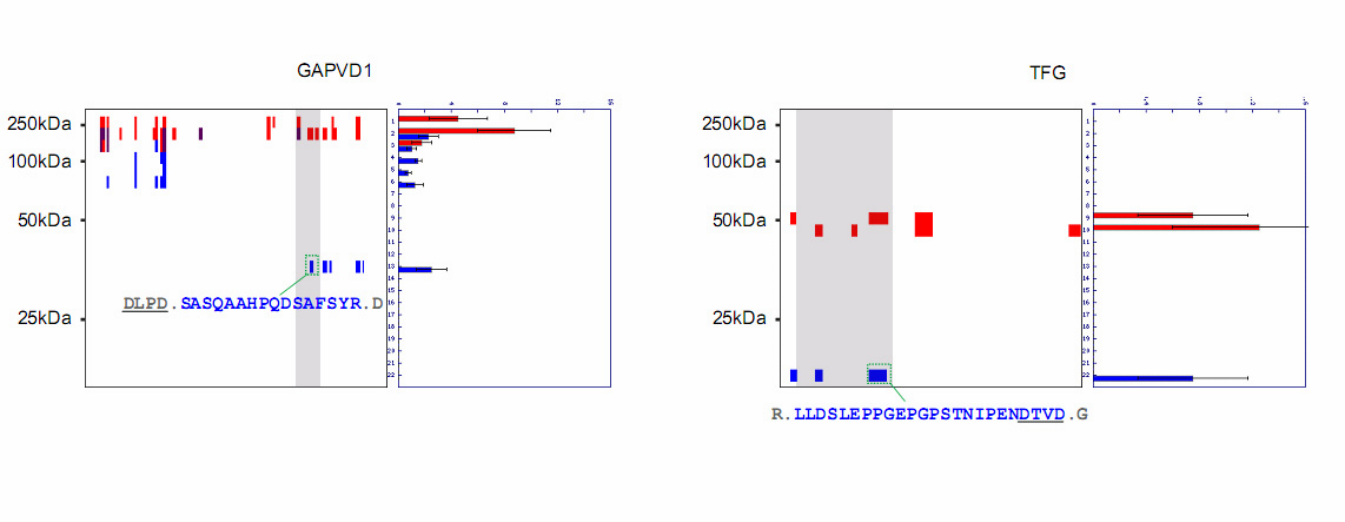

Figure S9. Peptographs for GAPVD1 and TFG Showing Precise Sites-of-Cleavage Identified by PROTOMAP

A previous mRNA-display study was able to identify regions of GAPVD1 and TFG that contained multiple potential sites-of-cleavage (shaded boxes) (Ju et al., 2007). The sequence coverage provided by PROTOMAP enabled the identification of the precise sites of caspase cleavage (D1112 and D142 for GAPVD1 and TFG, respectively).

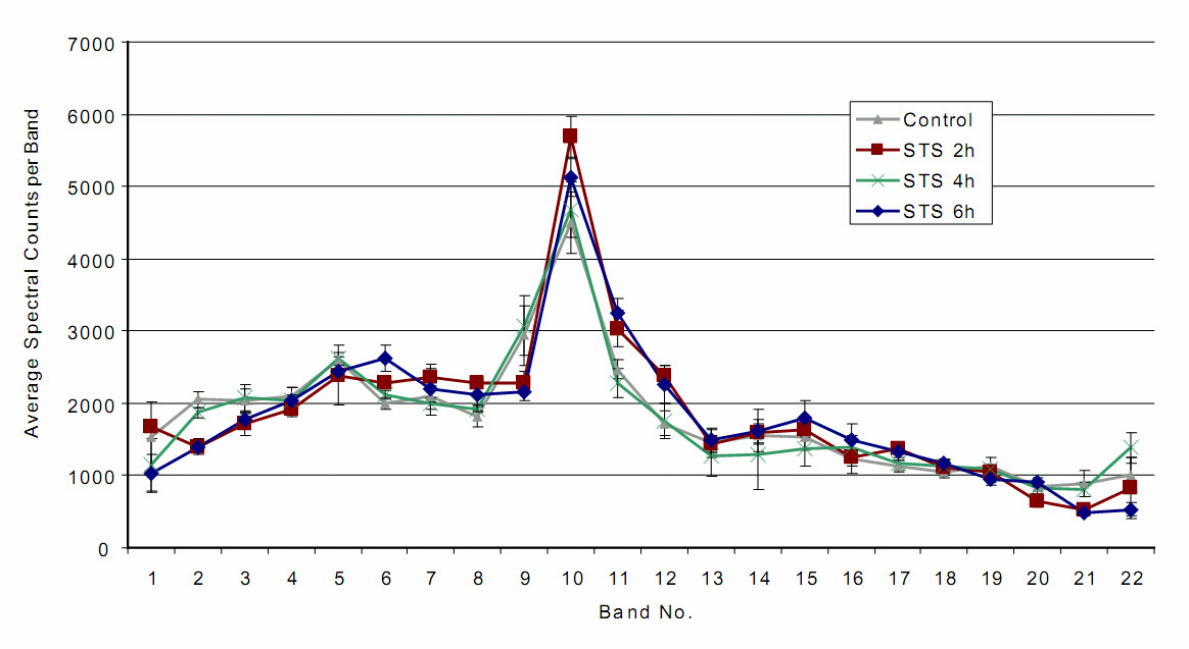

Figure S10. Reproducibility of PROTOMAP

The graph shows average total spectral-counts acquired in each band from each of the four datasets showing high overall reproducibility. Error bars represent standard error of the mean. Control and 'STS 4h' datasets were conducted with n=4 whereas 2 hr and 6 hr timepoints were conducted with n=3 as described in the Supplemental Experimental Procedures.

Supplemental References

Elias, J.E., and Gygi, S.P. (2007). Target-decoy search strategy for increased confidence in large-scale protein identifications by mass spectrometry. Nat Meth *4*, 207-214.
Eng, J.K., McCormack, A.L., and Yates, J.R. (1994). An approach to correlate tandem mass spectral data of peptides with amino acid sequences in a protein database. Journal of the American Society for Mass Spectrometry *5*, 976-989.
Jessani, N., Liu, Y., Humphrey, M., and Cravatt, B.F. (2002). Enzyme activity profiles of the secreted and membrane proteome that depict cancer cell invasiveness. Proceedings of the National Academy of Sciences *99*, 10335-10340.
Ju, W., Valencia, C.A., Pang, H., Ke, Y., Gao, W., Dong, B., and Liu, R. (2007). Proteome-wide identification of family member-specific natural substrate repertoire of caspases. Proceedings of the National Academy of Sciences *104*, 14294-14299.
Rosenfeld, J., Capdevielle, J., Guillemot, J.C., and Ferrara, P. (1992). In-gel digestion of proteins for internal sequence analysis after one- or two-dimensional gel electrophoresis. Analytical Biochemistry *203*, 173-179.
Tabb, D.L., McDonald, W.H., and Yates, J.R. (2002). DTASelect and Contrast: Tools for Assembling and Comparing Protein Identifications from Shotgun Proteomics. J Proteome Res *1*, 21-26.
Van Damme, P., Martens, L., Van Damme, J., Hugelier, K., Staes, A., Vandekerckhove, J., and Gevaert, K. (2005). Caspase-specific and nonspecific in vivo protein processing during Fas-induced apoptosis. Nat Meth *2*, 771-777.